Research Article

Mechanisms of Laser-Induced Reactions of Stacked Benzene Molecules: A Semiclassical Dynamics Simulation and CASSCF Calculation

Kunxian Shu,[1] Jie Zhao,[1] Shuai Yuan,[1] Yusheng Dou,[2] and Glenn V. Lo[2]

[1] *Institute of Bioinformatics, Chongqing University of Posts and Telecommunications, Chongqing 400065, China*
[2] *Department of Physical Sciences, Nicholls State University, P.O. Box 2022, Thibodaux, LA 70310, USA*

Correspondence should be addressed to Shuai Yuan; yuanshuai@cqupt.edu.cn and Yusheng Dou; yusheng.dou@nicholls.edu

The response to ultrashort laser pulses of two stacked benzene molecules has been studied by semiclassical dynamics simulation; two typical pathways were found following excitation of one of the benzene molecules by a 25 fs (FWHM), 4.7 eV photon. With a fluence of 40.49 J/m^2, the stacked molecules form a cyclobutane benzene dimer; the formation of the two covalent bonds linking two benzenes occurs asynchronously after the excimer decays to electronic ground state. With a fluence of 43.26 J/m^2, only one bond is formed, which breaks about 50 fs after formation, followed by separation into the two molecules. The deformation of benzene ring is found to play an important role in the bond cleavage.

1. Introduction

The photocycloaddition reactions of unsaturated double bond complexes are of theoretical interest because these reactions are involved in DNA photodamage [1–4] and organic synthesis [5, 6]. The best known examples are the [2 + 2] photocycloaddition (forming either cyclobutanes or four-membered heterocycles) and excited state [4 + 4] cycloadditions that produce cyclooctadiene compounds.

Although quite (thermally) stable, benzene molecules can become quite reactive when being photoexcited; they can be transformed to benzvalene [7, 8] and fulvene when being excited to the first singlet (S_1) excited state or to Dewar benzene [9, 10] when being excited to the second singlet (S_2) excited state. Benzene can be involved in a photocycloaddition reaction with an alkene molecule. The reactions can be classified into three categories [5, 6]: [2 + 2] (or *ortho*), [3 + 2] (or *meta*), and [4 + 2] (or *para*) photocycloadditions. Photocycloadditions of benzene and an alkene are usually triggered by the photoexcitation of the benzene molecule. If the S_1 state of benzene is involved, only *meta* addition is allowed to occur in a concerted fashion according to molecular orbital symmetry rules [11, 12]. The formation of *ortho*- and *para*-cycloadducts can be interpreted as being due to (i) charge transfer processes, (ii) nonconcerted mechanism, and (iii) excitation to the S_2 state. Clifford et al. found [13] that for the benzene plus ethylene system cycloadditions could take place from S_1 state without barrier through a conical intersection (CI), which is common to all three cycloadducts. This low energy CI results from the formation of one C–C bond between benzene and ethylene. Their subsequent studies [14] suggest that CI seam between S_1 and S_0 could control chemical selectivity in the photocycloaddition of benzene and ethylene.

Cycloadditions, [4 + 2] and [4 + 4], are also observed between polycondensed aromatic compounds such as naphthalene, anthracene, and their derivatives. The [4 + 2] cycloaddition (photo-Diels-Alder reaction) [15–18] is frequently observed with naphthalene derivatives. [4 + 4] photocycloadditions are often observed in two-arene systems which are connected by a saturated bridge (such as –CH$_2$–CH$_2$–CH$_2$– or –CH$_2$–O–CH$_2$–). These bridge aromatic systems can undergo intramolecular [4 + 4] photocycloadditions to form "biplanemers," in which the two π systems are stacked face-to-face [19].

To date, the mechanism of cycloaddition among aromatic ring compounds has not been clearly characterized.

Rogachev and coworkers [20] performed a series of calculations involving benzene dimers in the ground state, but no studies have been made on the photochemical dimerization of benzene. In this paper, we studied photoinduced [2 + 2] cycloaddition of two-benzene system by semiclassical dynamic simulation. The simulation results provide detailed dynamics features for this process from photon excitation to the formation of product. The geometry at the conical intersection (CI) between the first singlet (S_1) excited state and ground state (S_0) was optimized by using completed active space self-consistent field (CASSCF) method to compare with other theoretical results.

2. Methodology

2.1. Semiclassical Dynamics Simulation. We carried out the dynamics simulations using the semiclassical electron-radiation-ion dynamics (SERID) method. In this approach, the valence electrons are calculated by the time-dependent Schrödinger equation while both the radiation field and the motion of the nuclei are treated by the classical approximation. A detailed description of this technique has been published elsewhere [21, 22] and only a brief review is given here. The one-electron states are updated by solving the time-dependent Schrödinger equation at each time step (typically 0.05 femtoseconds in duration) in a nonorthogonal basis,

$$i\hbar \frac{\partial \Psi_j}{\partial t} = \mathbf{S}^{-1} \cdot \mathbf{H} \cdot \Psi_j, \qquad (1)$$

where $\mathbf{S}$ is the overlap matrix for the atomic orbitals. The laser pulse is characterized by the vector potential $\mathbf{A}$, which is coupled to the Hamiltonian via the time-dependent Peierls substitution

$$H_{ab}\left(\mathbf{X} - \mathbf{X}'\right) = H_{ab}^0\left(\mathbf{X} - \mathbf{X}'\right) \exp\left(\frac{iq}{\hbar c}\mathbf{A} \cdot \left(\mathbf{X} - \mathbf{X}'\right)\right); \qquad (2)$$

here $H_{ab}(\mathbf{X} - \mathbf{X}')$ is the Hamiltonian matrix element for basis functions a and b on atoms at $\mathbf{X}$ and $\mathbf{X}'$, respectively, and $q = -e$ is the charge of the electron.

The Hamiltonian matrix elements, overlap matrix elements, and repulsive energy are calculated with the density-functional based tight bonding (DFTB) method. The DFTB method does have essentially the same strengths and limitations as time-dependent density-functional theory (TD-DFT). In particularly, the bonding is well described but the excited state energies are typically too low. For this reason, we matched the effective central photon energy of the laser pulse to the relevant density-functional (rather than experimental) excitation energy and this should not adversely affect the interpretation of the results. This model has been used in biologically relevant studies such as photoinduced dimerization of thymine [23] and cytosine [24] via [2 + 2] photocycloaddition reaction. All the results were found to be consistent with experimental observations. The formation of cyclobutane pyrimidine dimer may provide good references for [2 + 2] photocycloaddition of benzene.

In this technique, forces acting on nucleus or ions are computed by the Ehrenfest equation

$$M_l \frac{d^2 X_{l\alpha}}{dt^2}$$
$$= -\frac{1}{2} \sum_j \Psi_j^+ \cdot \left(\frac{\partial \mathbf{H}}{\partial X_{l\alpha}} - i\hbar \frac{1}{2} \frac{\partial \mathbf{S}}{\partial X_{l\alpha}} \cdot \frac{\partial}{\partial t}\right) \cdot \Psi_j - \frac{\partial U_{\text{rep}}}{\partial X_{l\alpha}}, \qquad (3)$$

where U_{rep} is effective nuclear-nuclear repulsive potential and $X_{l\alpha} = \langle \widehat{X}_{l\alpha} \rangle$ is the expectation value of the time-dependent Heisenberg operator for the α coordinate of the nucleus labeled by l (with $\alpha = x, y, z$). Equation (3) is obtained by neglecting the second and higher order terms of the quantum fluctuations $\widehat{X} - \langle \widehat{X}_{l\alpha} \rangle$ in the exact Ehrenfest theorem.

The present "Ehrenfest" principle is complementary to other methods based on different approximations, such as the full multiple spawning model developed by the Ben-Nun and Martínez [25]. The limitation of this method is that the simulation trajectory moves along a path dominated by averaging over all the terms in the Born-Oppenheimer expansion [26, 27],

$$\Psi^{\text{total}}\left(X_n, x_e, t\right) = \sum_i \Psi_i^n\left(X_n, t\right) \Psi_i^e\left(x_e, X_n\right), \qquad (4)$$

rather than following the time evolution of a single potential energy surface, which is approximately decoupled from all the others [26–29]. (Here X_n and x_e represent the sets of nuclear and electronic coordinates resp., and the Ψ_i^e are eigenstates of the electronic Hamiltonian at fixed X_n.) The strengths of the present approach include retention of all of the $3N$ nuclear degrees of freedom and the incorporation of the laser excitation as well as the subsequent deexcitation at an avoided crossing near a conical intersection.

2.2. CASSCF. Multiconfigurational self-consistent field (MCSCF) is a method in quantum chemistry used to generate qualitatively correct reference states of molecules in cases where Hartree-Fock (HF) and DFT are not adequate (e.g., for molecular ground states which are quasidegenerate with low lying excited states or in bond breaking situations). It uses a linear combination of configuration state functions (CSF) or configuration determinants to approximate the exact electronic wavefunction of an atom or molecule. In an MCSCF calculation, the set of coefficients of both the CSFs or determinants and the basis functions in the molecular orbitals are varied to obtain the total electronic wavefunction with the lowest possible energy. This method can be considered a combination of configuration interaction (where the molecular orbitals are not varied but the expansion of the wave function are varied) and Hartree-Fock (where there is only one determinant but the molecular orbitals are varied). A particularly important MCSCF approach is the CASSCF, where the linear combination of CSFs includes all that arise from a particular number of electrons in a particular number of orbitals [30, 31].

In this research, the CASSCF *ab initio* computations used a 12-electron and 12-orbital active space involving all
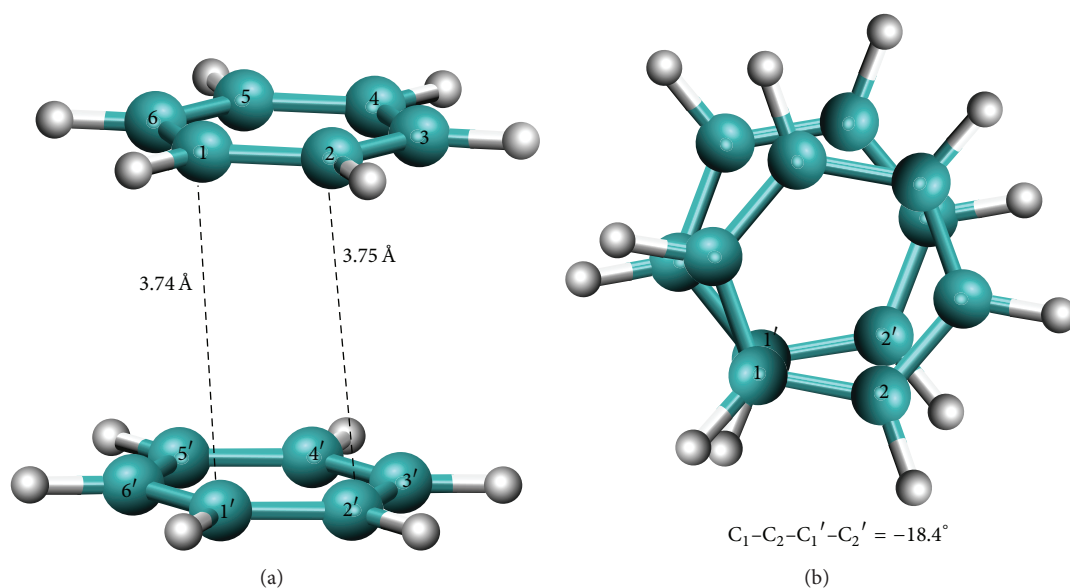
(a)

(b)

$C_1-C_2-C_1{}'-C_2{}' = -18.4°$

FIGURE 1: Conformation and atomic labeling for the stacked benzene system.

the π-orbitals of two benzene moieties. All the geometries were optimized using the 6–31G(d) basis set in Gaussian09 software package [32]. To enhance calculation efficiency, the geometry at the decay time in simulation trajectory was picked as the initial guess for CI optimization.

3. Results and Discussions

From the reported experiments and *ab initio* calculations [33–37], the ground state of two stacked benzenes can have two nearly isoenergetic stable structures (T-shaped and slipped-parallel) and a less stable sandwich structure. Electrostatic interaction stabilizes the T-shaped structure, while dispersion stabilizes the slipped-parallel structure. The initial structure used in our calculations, shown in Figure 1, is slipped parallel. Primed and unprimed labels are used to differentiate atoms in the two molecules. We fixed the $C_1-C_1{}'$ and $C_2-C_2{}'$ distances based on the geometries of [2 + 2] cycloaddition of hexatomic pyrimidine base [23, 24].

To obtain ground state equilibrium configurations of two benzene-system, the simulation was run at room temperature for 1000 fs, an "equilibrated" geometry was taken at twenty equal time intervals over the 1000 fs time period, and each one was excited with the laser pulse to generate the trajectories. A 25 fs FWHM laser pulse with a Gaussian profile, and 4.7 eV photon energy, was applied to the top benzene molecule. The selected photon energy matches the calculated HOMO-LUMO energy gap. A fluence between 10 and 50 J/m^2 was randomly chosen for this study. This fluence results in an electronic excitation but the forces produced do not break any bonds. The same laser pulse (Case 1: 40.49 J/m^2 fluence; Case 2: 43.26 J/m^2 fluence) is used for all 20 trajectories; one representative trajectory is reported in this paper. The other trajectories have similar results with the representative one.

Figure 2 shows the HOMO−1, HOMO, LUMO, and LUMO+1 for the equilibrated structure computed by the

DFTB approximation. Based on Woodward-Hoffmann rules, the formation of cyclobutane benzene dimer is a symmetry-forbidden reaction when both molecules are at the electronic ground states or have one electron promoted from the HOMO to the LUMO. However, the reaction is symmetry-allowed when one molecule is at electronic ground state and another one has one electron excited from the HOMO to the LUMO. These are evident from the molecular orbital diagram.

Case 1. Formation of cyclobutane benzene dimer.

In this section, we present and discuss the simulation results for the formation of cyclobutane benzene dimer. Six snapshots taken from the simulation at different times are shown in Figure 3. Figure 3(a) represents electronic excitation of the top molecule in the equilibrated geometry at 0 fs. The excited molecule is distorted (Figure 3(b)) and moves toward the unexcited molecule (Figure 3(c)). The unexcited molecule is deformed due to the approach of the excited molecule (Figure 3(d)). At 770 fs, $C_1-C_1{}'$ bond has been formed (Figure 3(e)). The second bond, $C_2-C_2{}'$, is formed at 1000 fs (Figure 3(f)). The structure of cyclobutane benzene remains stable by the end of the simulation.

The variations with time of the lengths of the C_1-C_2 and $C_1{}'-C_2{}'$ bonds and the distances of $C_1-C_1{}'$ and $C_2-C_2{}'$ are presented in Figure 4. Both C_1-C_2 and $C_1{}'-C_2{}'$ bonds are double bonds in the benzene molecules but become single bonds in the benzene dimer. The C_1-C_2 bond length starts at about 1.4 Å, typical for a C=C double bond in an arene, and then lengthens after the laser pulse is applied. The excited benzene molecule approaches the unexcited benzene molecule and influences its structure, as shown by the increase in the $C_1{}'-C_2{}'$ bond length after 200 fs. Both bond lengths increase to about 1.5 Å after 600 fs, because of the formation of the cyclobutane benzene dimer, and they remain at this length until the end of the simulation. Both
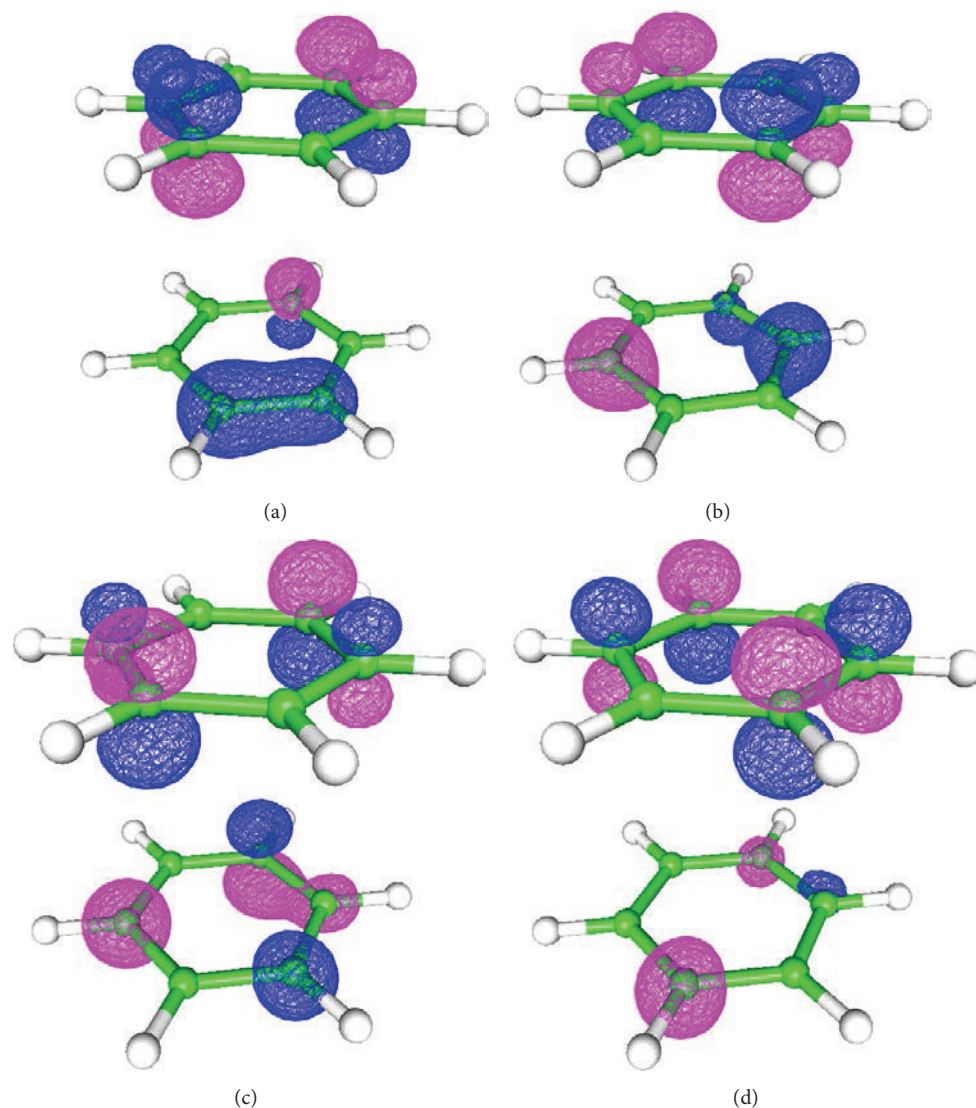
(a)   (b)

(c)   (d)

FIGURE 2: The diagrams of the (a) HOMO−1 (b), HOMO, (c) LUMO, and (d) LUMO + 1 of two stacked benzene molecules at the equilibrated geometry.

distances roughly remain at their initial values by 200 fs and start to decrease thereafter. The $C_1–C_1'$ distance decreases to below 1.5 Å at about 770 fs. The $C_2–C_2'$ distance drops to about 2.1 Å at about 830 fs, retains this value for 170 fs, and then drops to about 1.5 Å at about 1000 fs. This is the time for the formation of the cyclobutane benzene dimer.

The variations with time of the HOMO−1, HOMO, LUMO, and LUMO+1 energies are shown in Figure 5 along with the time-dependent population of the orbitals. Note that the HOMO and HOMO−1 are initially two identical HOMOs of the benzene monomer molecules and the LUMO and LUMO+1 are initially two identical LUMOs of the two molecules before laser excitation. Figure 5(a) shows that there is an abrupt change in the LUMO energy soon after application of the laser pulse. The HOMO and LUMO levels find one close approach, with avoided crossings, with the energy gaps being 0.04 eV at 770 fs. Figure 5(b) shows that by the end of the laser pulse (which is 50 fs) about 1 electron is excited from

the HOMO to the LUMO, consistent with the promotion of one benzene molecule to an electronically excited state. The coupling between the HOMO and LUMO, as observed in Figure 5(a), leads to notable electronic transitions from the LUMO to the HOMO. This deexcitation eventually brings the molecule to the electronic ground state. It can be seen from Figure 6 that shortly after the coupling both the LUMO and HOMO levels move toward their initial values. After 1000 fs, when the formation of the cyclobutane benzene dimer is completed, these two energy levels only show fluctuations about constants values, which are essentially the same as their initial values. On the other hand, the LUMO+1 and HOMO−1 levels only show slight variations during the reaction, since they are the LUMO and HOMO of the unexcited molecule, respectively.

Case 2. Formation and subsequent cleavage of only one σ-bond between the two benzene molecules.
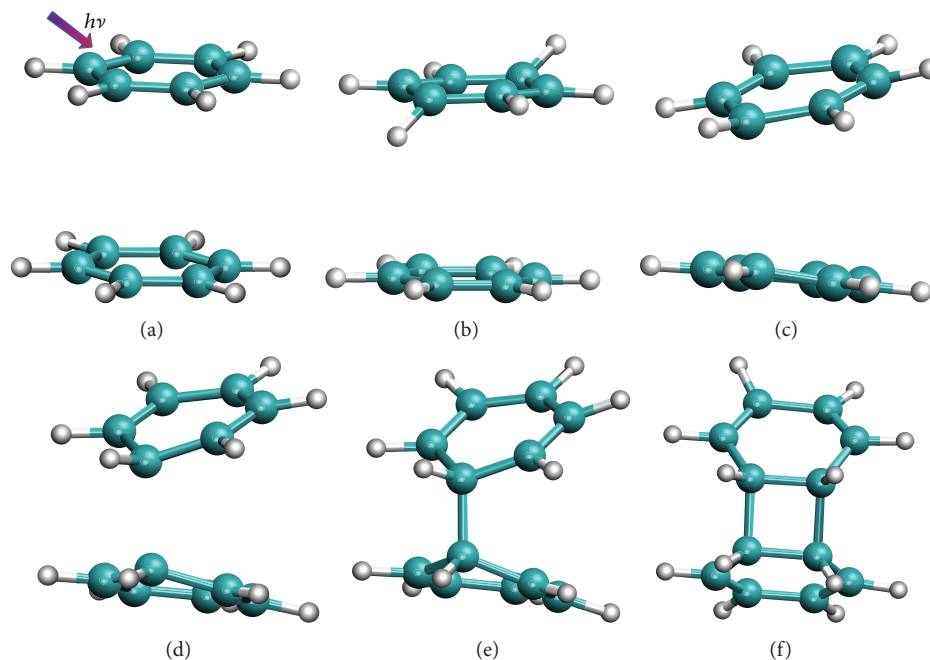
FIGURE 3: Snapshots taken from the simulation of two stacked benzene molecules at (a) 0, (b) 300, (c) 700, (d) 740, (e) 770, and (f) 1000 fs. The molecule at the top is subjected to the irradiation of a 25 fs (fwhm) laser pulse with a fluence of 40.49 J·m^{-2} and photon energy of 4.7 eV. This trajectory leads to the formation of cyclobutane benzene dimer and is briefly defined as Case 1.
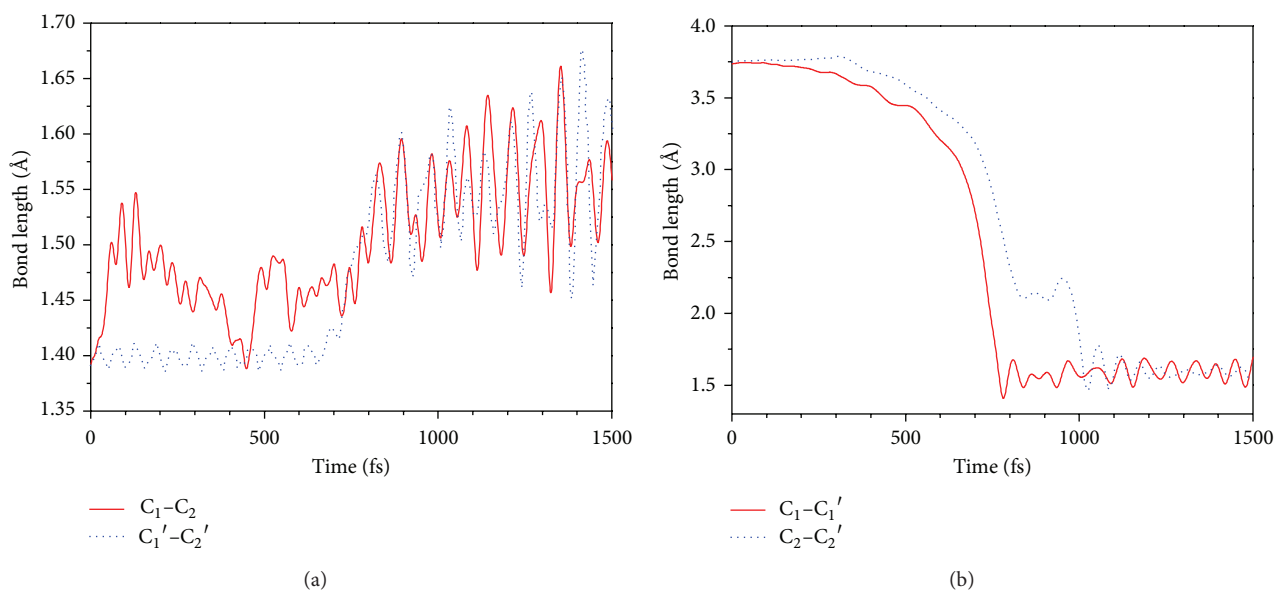

FIGURE 4: The variations with time of (a) C_1-C_2 and $C_1'-C_2'$ bond lengths and (b) the lengths between the C_1 and C_2 atoms and the C_1' and C_2' atoms in two stacked benzene molecules in Case 1.

The simulation results presented in this section show that under the laser irradiation two molecules form a σ bond between the C_1 and C_1' atom sites. However, this σ bond only has a lifetime of several ten femtoseconds and breaks shortly after it is formed.

Six snapshots taken from the simulation at different times are shown in Figure 6. One finds that at 930 fs two molecules have already formed a chemical bond between the C_1 and C_1' atoms (Figure 6(d)) but the bond breaks shortly thereafter and the two molecules move away from each other (Figures 6(e) and 6(f)).

The variations with time of the C_1-C_2 and $C_1'-C_2'$ bond lengths are plotted in Figure 7(a). The C_1-C_2 bond stretches in length soon after the laser pulse is applied due to the excitation of electrons from the HOMO to LUMO and shrinks to its original length shortly after 900 fs when the
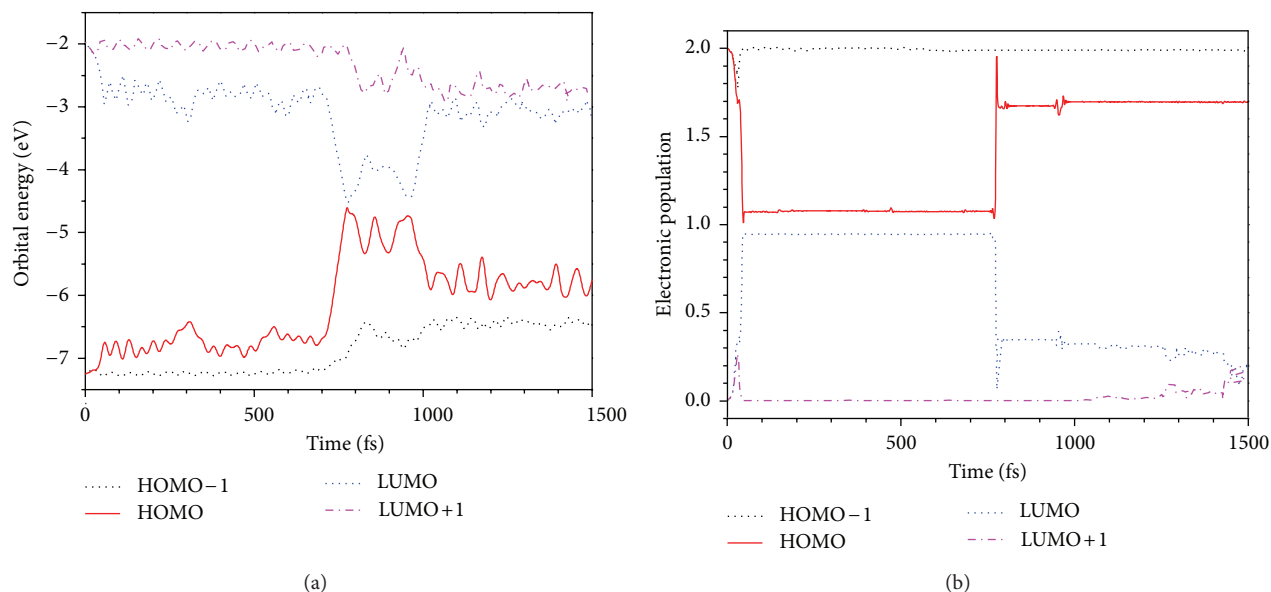
(a)

(b)

FIGURE 5: The variations with time of (a) orbital energies and (b) time-dependent populations of the HOMO−1, HOMO, LUMO, and LUMO+1 of two benzene molecules in Case 1.
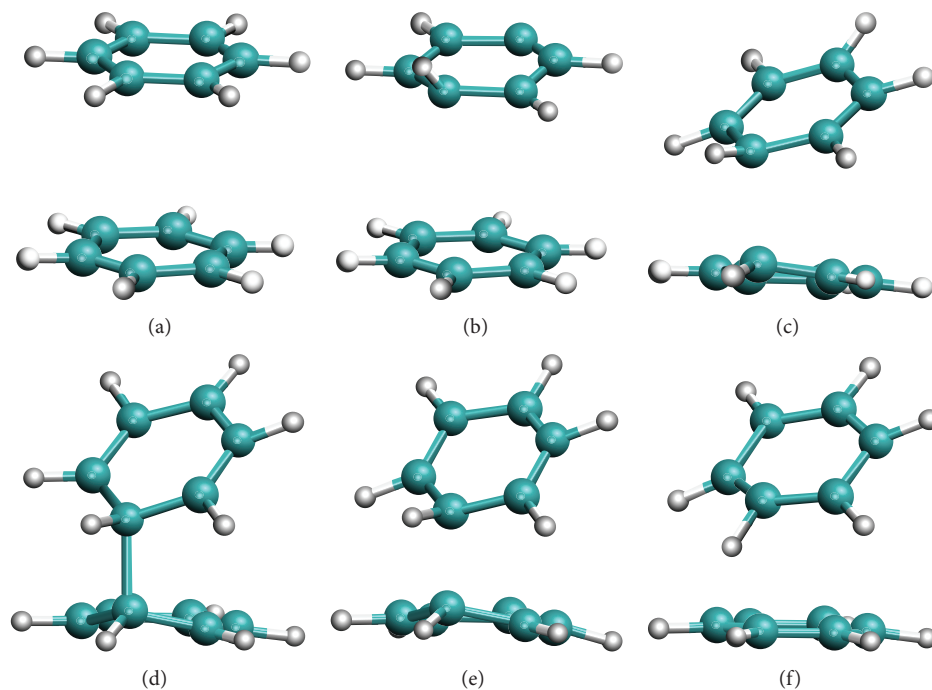

FIGURE 6: Snapshots taken from the simulation of two stacked benzene molecules at (a) 0, (b) 350, (c) 790, (d) 930, (e) 960, and (f) 1100 fs. The molecule at the top is subjected to the irradiation of a 25 fs (fwhm) laser pulse with a fluence of 43.26 J·m^{-2} and photon energy of 4.7 eV. This trajectory results in the breaking of C_1–C_1' bond and is briefly defined as Case 2.

bond linking two benzene molecules is broken. However, the C_1'–C_2' bond shows little variation since excitation. A sharp jump up and down in the C_1'–C_2' bond length during 900 to 1000 fs indicates the formation and breakage of the bond between two benzene molecules. The variations with time of the C_1–C_1' and C_2–C_2' distances are plotted in Figure 7(b) for this process. Both distances do not exhibit significant

changes until 400 fs but show a decrease afterwards due to the interaction between two close molecules. The C_1–C_1' distance becomes about 1.5 Å at about 930 fs, indicating the formation of a C–C σ-bond. Immediately after that, the distances between the C_1 and C_1' atoms and the C_2 and C_2' atoms increase quickly because two molecules separated from each other.
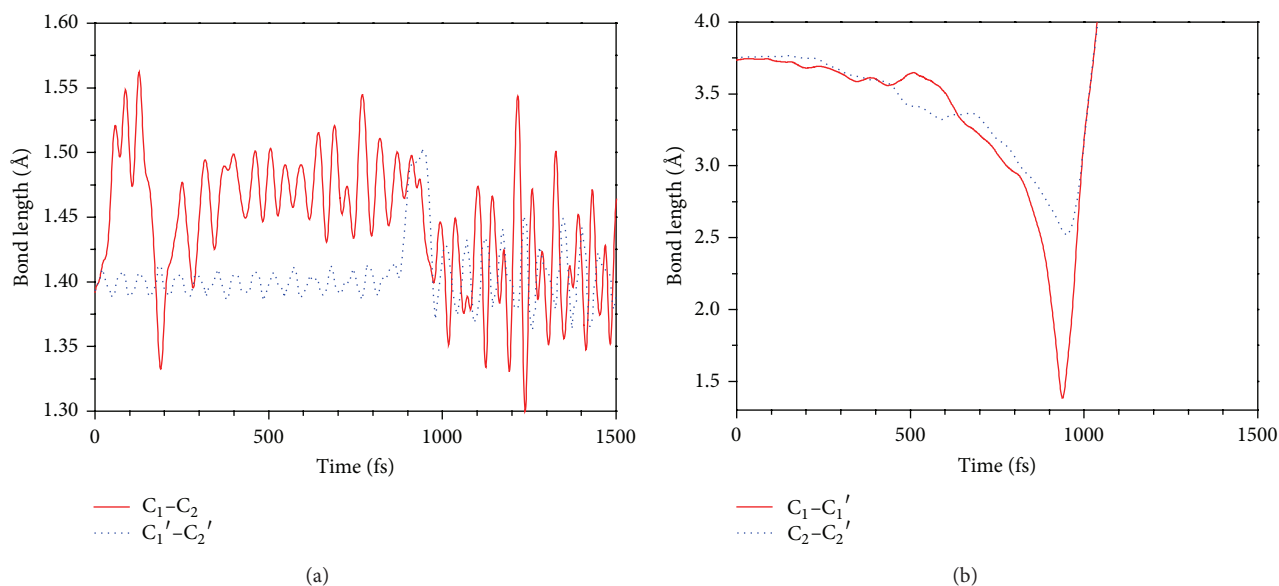
(a)

(b)

FIGURE 7: The variations with time of (a) C_1–C_2 and C_1'–C_2' bond lengths and (b) the lengths between the C_1 and C_2 atoms and the C_1' and C_2' atoms in two stacked benzene molecules in Case 2.
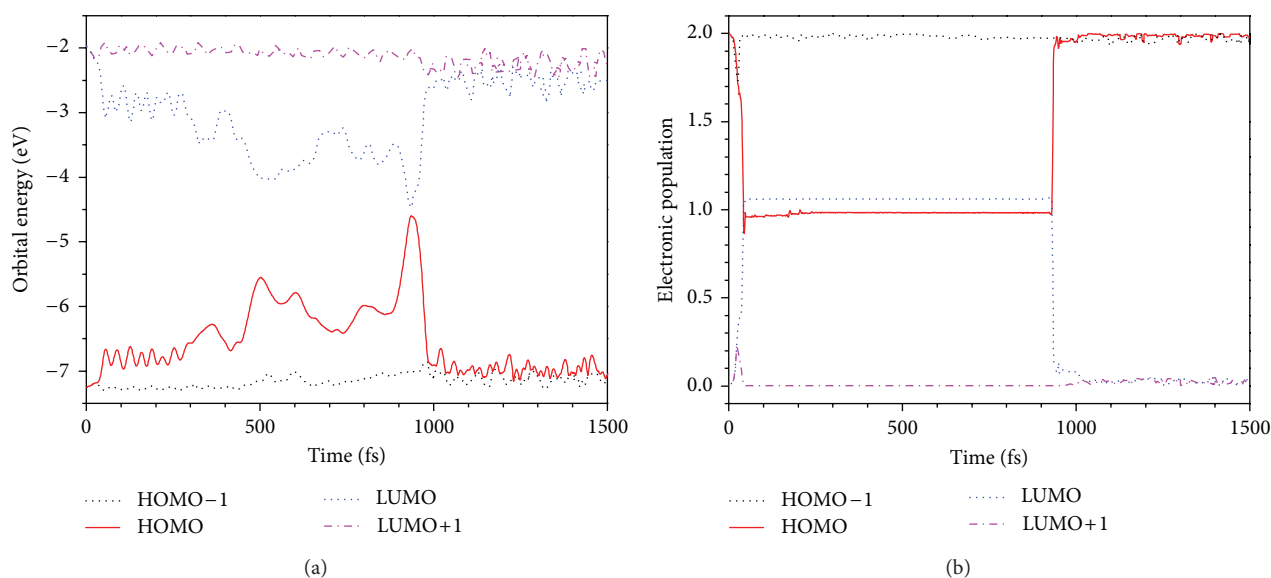

(a)

(b)

FIGURE 8: The variations with time of (a) orbital energies and (b) time-dependent populations of the HOMO−1, HOMO, LUMO, and LUMO+1 of two benzene molecules in Case 2.

The variations of the HOMO−1, HOMO, LUMO, and LUMO+1 energies as a function of time are shown in Figure 8(a) and the time-dependent populations of the HOMO and LUMO are shown in Figure 8(b). An avoided crossing between the HOMO and LUMO levels is found with the energy gaps being 0.05 eV at 605 fs. This avoided crossing leads to notable electronic transition from the LUMO to HOMO, which eventually directs the excimer to the electronic ground state.

3.1. Discussion. It is seen from Figures 4, 5, 7, and 8 that the formation of the C_1–C_1' and C_2–C_2' bonds has a crucial impact on the nonadiabatic transition of the excimer to the electronic ground state. In addition, the deformation of the benzene ring, especially the deformation of the benzene rings at C_1, C_2, C_1', and C_2' atoms sites, also has a notable influence on the nonadiabatic transition of the excimer to ground state. To understand this, a comparison between the C_5–C_6–C_1–C_2 and C_5'–C_6'–C_1'–C_2' dihedral angles and the energy gap between the HOMO and LUMO for each case is plotted in Figure 9. The deformation of the benzene ring at the C_1, C_2, C_1', and C_2' atoms sites is represented by these two dihedral angles. It is seen that, for each case, the minimum of the energy gap is in line with a sharp rise of the C_5'–C_6'–C_1'–C_2'
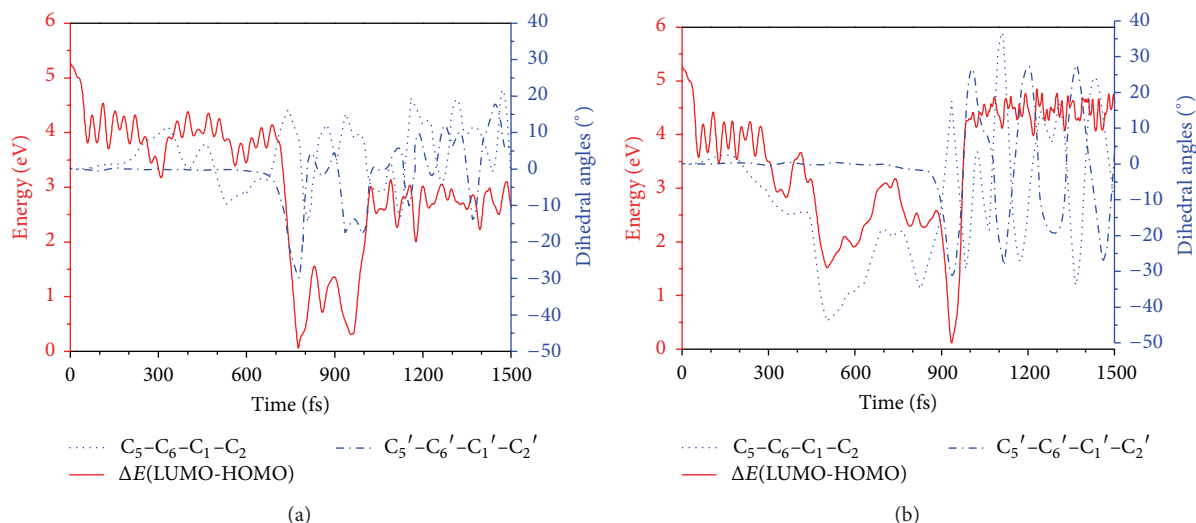
FIGURE 9: Comparison between the C_5–C_6–C_1–C_2 and $C_5{}'$–$C_6{}'$–$C_1{}'$–$C_2{}'$ dihedral angles and the energy gap between the HOMO and LUMO of two stacked benzene molecules: (a) Case 1 and (b) Case 2.

dihedral angle and a sharp dip in the C_5–C_6–C_1–C_2 dihedral angle, suggesting that in both cases the deformation of the benzene ring plays an important role in the nonadiabatic transition of the excimer to ground state.

In Case 2 the C_1–$C_1{}'$ bond between two benzenes is broken about 50 fs after its formation. To understand how the structural deformation of the benzene ring impacts the cleavage of the C_1–$C_1{}'$ bond, it is worthwhile to the compare the distances between the C_1 and $C_1{}'$ atoms and the C_2 and $C_2{}'$ atoms and the C_5–C_6–C_1–C_2 and $C_5{}'$–$C_6{}'$–$C_1{}'$–$C_2{}'$ dihedral angles. For the formation of the cyclobutane benzene dimer, the dihedral angle of $C_5{}'$–$C_6{}'$–$C_1{}'$–$C_2{}'$ is almost constant before 680 fs (i.e., just before the formation of the C_1–$C_1{}'$ bond) and then quickly decreases to $-30°$. After that, this dihedral angle fluctuates around its initial value until the end of simulation. On the other hand, the dihedral angle of C_5–C_6–C_1–C_2 has a relatively smaller change in amplitude. In particular, during 770 to 1050 fs, in which the C_1–$C_1{}'$ bond is formed and C_2–$C_2{}'$ is not bonding, the value of C_5–C_6–C_1–C_2 dihedral angle is dominantly positive. This suggests movement of C_1 and C_2 towards the bottom molecule, enhancing the likelihood of C_2–$C_2{}'$ bonding. For Case 2, however, the C_5–C_6–C_1–C_2 dihedral angle oscillates between $-30°$ and $30°$ after formation of the C_1–$C_1{}'$ bond. This strong vibration deters the formation of a bond between the C_2 and $C_2{}'$ and also makes the C_1–$C_1{}'$ bond unstable. We therefore conclude that the forces produced by the deformation of the benzene ring at C_1 site break the C_1–$C_1{}'$ bond and prevent the formation of the cyclobutane benzene dimer.

The time evolution of the net charge of the excited benzene molecule (benzene 1) in Cases 1 and 2 is shown in Figures 10(a) and 10(c), respectively. Figure 10(b) is an expanded view of Figure 10(a) from 600 to 1100 fs, with C_1–$C_1{}'$ and C_2–$C_2{}'$ distances shown for comparison. Figure 10(d) is an expanded view of Figure 10(c) from 800 to 1000 fs, with C_1–$C_1{}'$ and C_2–$C_2{}'$ distances also shown for

comparison. For the formation of the cyclobutane benzene dimer (Case 1), although electrons hop frequently between the two benzene molecules from 700 to 1000 fs, it can be hardly defined as "charge transfer state" overall. Only at 770 fs, when the avoided crossing occurs, a zwitterion is clearly formed. However, the excited benzene molecule almost immediately returns to electric neutrality. In the zwitterionic geometry, C_1 and $C_1{}'$ atoms are linked by a σ chemical bond with length of 1.58 Å, while the C_2 and $C_2{}'$ distance is 2.66 Å. A "bonded-intermediate" is almost immediately formed as the C_2–$C_2{}'$ distance shortens from 2.6 to about 2.1 Å. After 1000 fs, the bonded-intermediate has converted into the cyclobutane benzene dimer because of C_2–$C_2{}'$ bonding. In Case 2, as shown in Figures 10(c) and 10(d), the zwitterionic exists for about 20 fs and then C_1–$C_1{}'$ bond is broken. The bonded-intermediate is not observed in Case 2.

The molecular geometry at the avoided crossing of both cases is shown in Figure 11 with a few critical geometry parameters indicated. The distances of C_1–$C_1{}'$ and C_2–$C_2{}'$ of Case 1 are 1.58 and 2.66 Å, respectively. The interatomic distances of Case 2 are 1.57 and 2.61 Å, respectively. Figures 11(a) and 11(b) are not significantly different. It suggests that the electronic decay point, which is bonded-intermediate structure, may lead to either [2 + 2] photoaddition product or reversal, depending on the vibrations of C_1, C_2, $C_1{}'$, and $C_2{}'$ atoms.

The interatomic distances of C_1–$C_1{}'$ and C_2–$C_2{}'$ are 1.64 Å and 2.60 Å, respectively, (as seen in Figure 12) by using CASSCF optimization for the S_1/S_0 CI of two-benzene system. It is worth noting that the C_3–$C_2{}'$ distance in the CI geometry is only 2.21 Å, which is far less than that obtained in our semiclassical dynamics simulations (both Cases 1 and 2). This CASSCF geometry is very similar to the CI of benzene and ethylene system calculated by Clifford and coworkers [13]. Decay from this CI point may lead to either [2 + 2], [2 + 3], or [2 + 4] photoaddition product, although formation
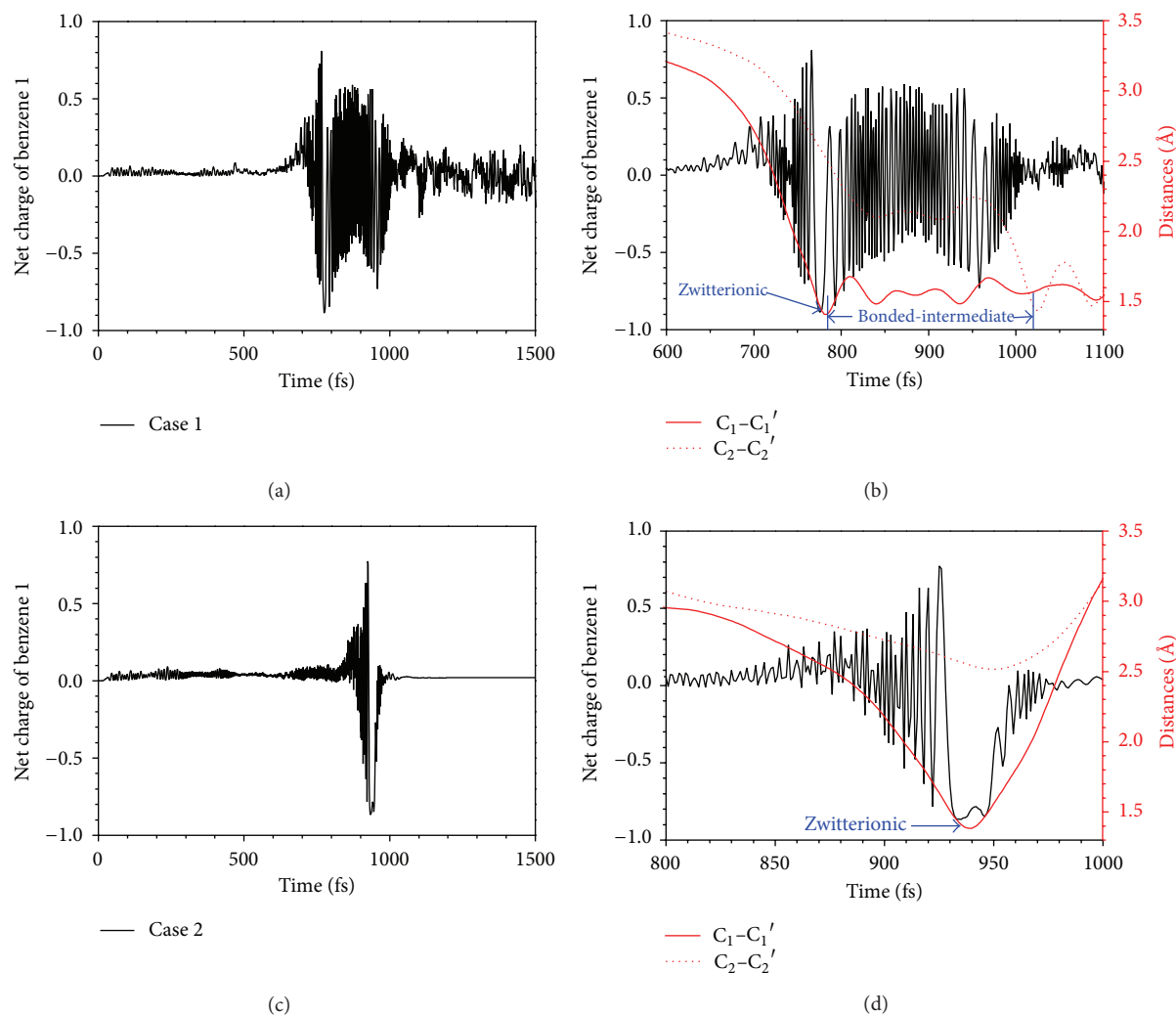
(a)

(b)

(c)

(d)

FIGURE 10: The net charge of benzene 1 molecule of (a) Case 1 and (c) Case 2. Here (b) is the detail of (a) from 600 to 1200 fs and both C_1–C_1' and C_2–C_2' distances are inserted to compare; (d) is the expanded scale of (c) from 800 to 1000 fs and both C_1–C_1' and C_2–C_2' distances in that case are inserted.

of [2 + 3] product seems most probable because of the short C_3–C_2' distance.

Classical photoinduced [2 + 2] cycloadditions proceed via a cyclic transition state and are concerted reactions, in which bond breaking and bond formation take place simultaneously and no intermediate state is involved. But for the photoinduced [2 + 2] dimerization of benzenes, our simulation results show that the C_1–C_1' and C_2–C_2' bond formations are nonconcerted. The CASSCF calculation suggests that two stacked benzenes decay to the electronic ground state via the CI when the formation of the C_1–C_1' bond occurs and that the C_2–C_2' distance is longer than C_1–C_1' at the CI. Therefore, the Woodward-Hoffmann rules do not apply. Our simulations suggest the formation of a "bonded-intermediate" at avoided crossing; it involves a charge separation leading to a zwitterion and a "bonded-intermediate." The bonded-intermediate is a necessary intermediate for forming [2 + 2] product. Otherwise, the zwitterion could reverse to reactant with the breaking of the C_1–C_1' bond.

4. Conclusions

In this paper, we report a semiclassical dynamics simulation study of the response to ultrashort laser pulses of stacked benzene molecules. The simulation uncovered two different reaction paths, leading to the formation of two different products. The first leads to the formation of cyclobutane benzene dimer and the second eventually returns back to reactants after deactivation. The simulation results can be summarized as follows.

(1) In both reactions, the distances between the C_1 and C_1' atoms have a great impact on the formation of the avoided crossings, which lead to the deactivation of the photoexcited molecule. Radiationless transformation of both cases occurs when the C_1 and C_1' atoms form a covalent bond.

(2) In the first reaction, the formation of the two chemical bonds is asynchronous and a time lag is 230 fs. A

$C_2–C_1–C_1{}'–C_2{}' = 19.5°$

(a)

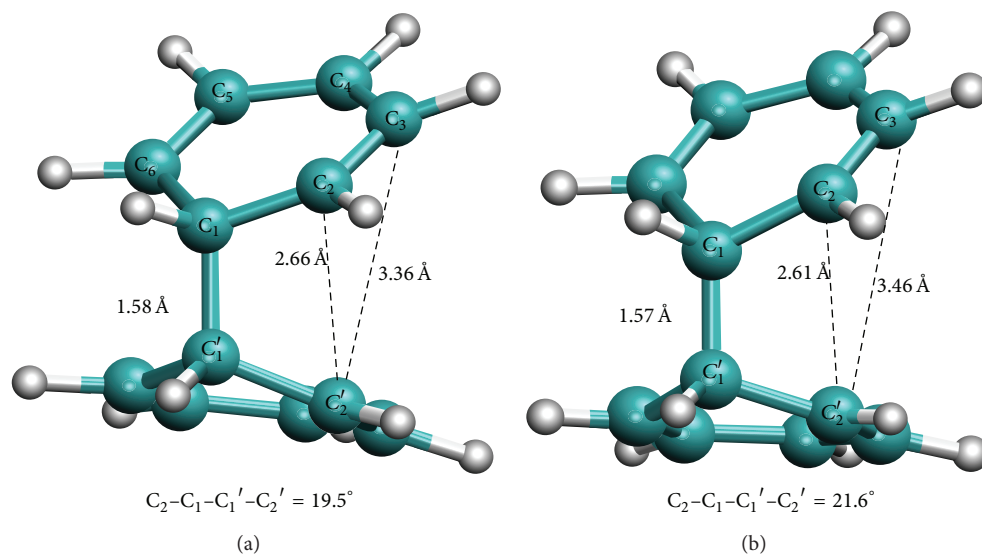$C_2–C_1–C_1{}'–C_2{}' = 21.6°$

(b)

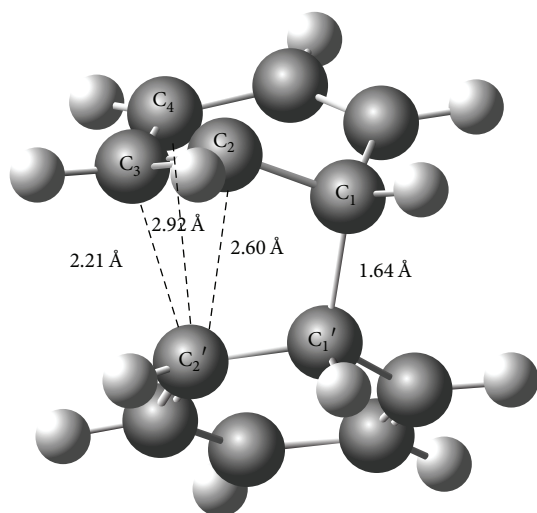Figure 11: The molecular geometry at avoided crossing of (a) Case 1 and (b) Case 2.

Figure 12: The geometry of conical intersection by CASSCF(12,12)/6–31g(d) optimization.

bonded-intermediate is observed before the formation of cyclobutane dimer.

(3) In the second reaction, only one bond is formed between two benzene molecules. This bonded-intermediate exists for only 50 fs and possesses significant zwitterionic character. The final product is two separated benzene molecules. The deformation of benzene ring plays an important role in the breaking of this bond.

Conflict of Interests

The authors declare that there is no conflict of interests regarding the publication of this paper.
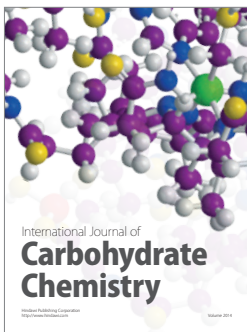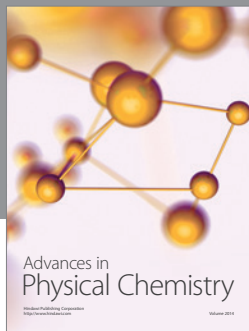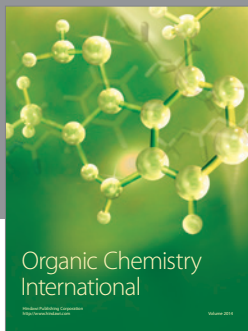
References

[1] R. Beukers, A. P. M. Eker, and P. H. M. Lohman, "50 years thymine dimer," *DNA Repair*, vol. 7, no. 3, pp. 530–543, 2008.

[2] C. E. Crespo-Hernández, B. Cohen, and B. Kohler, "Base stacking controls excited-state dynamics in A-T DNA," *Nature*, vol. 436, pp. 1141–1144, 2005.

[3] C. T. Middleton, K. de la Harpe, C. Su, Y. K. Law, C. E. Crespo-Hernández, and B. Kohler, "DNA excited-state dynamics: from single bases to the double helix," *Annual Review of Physical Chemistry*, vol. 60, pp. 217–239, 2009.

[4] M. Boggio-Pasqua, G. Groenhof, L. V. Schäfer, H. Grubmüller, and M. A. Robb, "Ultrafast deactivation channel for thymine dimerization," *Journal of the American Chemical Society*, vol. 129, no. 36, pp. 10996–10997, 2007.

[5] N. Hoffmann, "Photochemical reactions as key steps in organic synthesis," *Chemical Reviews*, vol. 108, pp. 1052–1103, 2008.

[6] U. Streit and C. G. Bochet, "The arene-alkene photocycloaddition," *Beilstein Journal of Organic Chemistry*, vol. 7, pp. 525–542, 2011.

[7] K. E. Wilzbach, J. S. Ritscher, and L. Kaplan, "Benzvalene, the tricyclic valence isomer of benzene," *Journal of the American Chemical Society*, vol. 89, no. 4, pp. 1031–1032, 1967.

[8] L. Kaplan and K. E. Willzbach, "Photolysis of benzene vapor. Benzvalene formation at wavelengths 2537–2370 A," *Journal of the American Chemical Society*, vol. 90, no. 12, pp. 3291–3292, 1968.

[9] E. E. van Tamelen and S. P. J. Pappas, "Chemistry of dewar benzene. 1,2,5-Tri-t-butylbicyclo[2.2.0]Hexa-2,5-diene," *Journal of the American Chemical Society*, vol. 84, pp. 3789–3791, 1962.

[10] E. E. van Tamelen and S. P. Pappas, "Bicyclo[2.2.0]hexa-2,5-diene [3]," *Journal of the American Chemical Society*, vol. 85, no. 20, pp. 3297–3298, 1963.

[11] D. Bryce-Smith, "Orbital symmetry relationships for thermal and photochemical concerted cycloadditions to the benzene ring," *Journal of the Chemical Society D*, no. 14, pp. 806–808, 1969.

[12] J. A. van der Hart, J. J. C. Mulder, and J. Cornelisse, "Funnels and barriers in the photocycloaddition of arenes to alkenes and dienes," *Journal of Photochemistry and Photobiology A*, vol. 86, no. 1–3, pp. 141–148, 1995.

[13] S. Clifford, M. J. Bearpark, F. Bernardi, M. Olivucci, M. A. Robb, and B. R. Smith, "Conical intersection pathways in the photocycloaddition of ethene and benzene: a CASSCF study with MMVB dynamics," *Journal of the American Chemical Society*, vol. 118, no. 31, pp. 7353–7360, 1996.

[14] J. J. Serrano-Pérez, F. de Vleeschouwer, F. de Proft, D. Mendive-Tapia, M. J. Bearpark, and M. A. Robb, "How the conical intersection seam controls chemical selectivity in the photocycloaddition of ethylene and benzene," *Journal of Organic Chemistry*, vol. 78, no. 5, pp. 1874–1886, 2013.

[15] J. J. McCullough, "Photoadditions of aromatic compounds," *Chemical Reviews*, vol. 87, no. 4, pp. 811–860, 1987.

[16] D. Döpp, "Photocycloaddition with captodative alkenes," in *Organic, Physical and Materials Photochemistry*, V. Ramamurthy and K. S. Schanze, Eds., vol. 6 of *Molecular and Supramolecular Photochemistry*, pp. 101–148, Marcel Dekker, New York, NY, USA, 2000.

[17] K. Mizuno, H. Maeda, A. Sugimoto, and K. Chiyonobu, "Molecular and supramolecular photochemistry," in *Understanding and Manipulating Excited-State Processes*, V. Ramamurthy and K. S. Schanze, Eds., vol. 8, p. 127, Marcel Dekker, New York, NY, USA, 2001.

[18] D. Döpp, C. Krüger, H. R. Memarian, and Y.-H. Tsay, "1,4-photocycloaddition of α-morpholinoacrylonitrile to 1-acylnaphthalenes," *Angewandte Chemie International Edition in English*, vol. 24, no. 12, pp. 1048–1049, 1985.

[19] H. Meier and D. Cao, "Optical switches with biplanemers obtained by intramolecular photocycloaddition reactions of tethered arenes," *Chemical Society Reviews*, vol. 42, pp. 143–155, 2013.

[20] A. Y. Rogachev, X.-D. Wen, and R. Hoffmann, "Jailbreaking benzene dimers," *Journal of the American Chemical Society*, vol. 134, no. 19, pp. 8062–8065, 2012.

[21] Y. Dou, B. R. Torralva, and R. E. Allen, "Semiclassical electron-radiation-ion dynamics (SERID) and cis-trans photoisomerization of butadiene," *Journal of Modern Optics*, vol. 50, no. 15–17, pp. 2615–2643, 2003.

[22] Y. Dou, B. R. Torralva, and R. E. Allen, "Gas phase absorption spectra and decay of triplet benzene, benzene-d_6, and toluene," *Chemical Physics Letters*, vol. 392, no. 4, pp. 352–358, 2004.

[23] W. Zhang, S. Yuan, A. Li, Y. Dou, J. Zhao, and W. Fang, "Photoinduced thymine dimerization studied by semiclassical dynamics simulation," *The Journal of Physical Chemistry C*, vol. 114, no. 12, pp. 5594–5601, 2010.

[24] S. Yuan, W. Zhang, L. Liu, Y. Dou, W. Fang, and G. V. Lo, "Detailed mechanism for photoinduced cytosine dimerization: a semiclassical dynamics simulation," *The Journal of Physical Chemistry A*, vol. 115, no. 46, pp. 13291–13297, 2011.

[25] M. Ben-Nun and T. J. Martínez, "Ab Initio quantum molecular dynamics," *Advances in Chemical Physics*, vol. 121, pp. 439–512, 2002.

[26] W. Domcke, D. R. Yarkony, and H. Koppel, Eds., *Conical Intersections: Electronic Structure, Dynamics, and Spectroscopy*, World Scientific, Singapore, 2004.

[27] M. Baer, *Beyond Born-Oppenheimer: Electronic Nonadiabatic Coupling Terms and Conical Intersections*, Wiley-Interscience, Hoboken, NJ, USA, 2006.

[28] M. J. Bearpark, F. Bernardi, S. Clifford, M. Olivucci, M. A. Robb, and T. J. Vreven, "The lowest energy excited singlet states and the cis-trans photoisomerization of styrene," *Journal of the American Chemical Society*, vol. 101, no. 2, pp. 3841–3847, 1997.

[29] B. G. Levine and T. J. Martínez, "Isomerization through conical intersections," *Annual Review of Physical Chemistry*, vol. 58, pp. 613–634, 2007.

[30] J. Frank, *Introduction to Computational Chemistry*, John Wiley & Sons, Chichester, UK, 2007.

[31] C. J. Cramer, *Essentials of Computational Chemistry*, John Wiley & Sons, Chichester, UK, 2002.

[32] M. J. Frisch, G. W. Trucks, H. B. Schlegel et al., *Gaussian 09, Revision D01*, Gaussian, Wallingford, Conn, USA, 2010.

[33] S. Tsuzuki, "Interactions with aromatic rings," *Structure and Bonding*, vol. 115, pp. 149–193, 2005.

[34] K. C. Janda, J. C. Hemminger, J. S. Winn, S. E. Novick, S. J. Harris, and W. Klemperer, "Benzene dimer: a polar molecule," *The Journal of Chemical Physics*, vol. 63, no. 4, pp. 1419–1421, 1975.

[35] J. M. Steed, T. A. Dixon, and W. Klemperer, "Molecular beam studies of benzene dimer, hexafluorobenzene dimer, and benzene-hexafluorobenzene," *The Journal of Chemical Physics*, vol. 70, no. 11, pp. 4940–4946, 1979.

[36] E. Arunan and H. S. Gutowsky, "The rotational spectrum, structure and dynamics of a benzene dimer," *The Journal of Chemical Physics*, vol. 98, no. 5, pp. 4294–4296, 1993.

[37] W. Scherzer, O. Kratzschmar, H. L. Selzle, and E. W. Schlag, "Structural isomers of the benzene dimer from mass selective hole-burning spectroscopy," *Zeitschrift für Naturforschung A*, vol. 47, pp. 1248–1252, 1992.